

# Numerical Simulation for Achieving Optimum Dimensions of a Solar Chimney Power Plant

M. Ghalamchi<sup>1,\*</sup>, M. Ghalamchi<sup>2</sup>, T. Ahanj<sup>3</sup>

<sup>1</sup>Department of Energy Engineering, Science and Research Campus, Islamic Azad University, Tehran, Iran

<sup>2</sup>Faculty of New Sciences & Technologies, University of Tehran, Tehran, Iran

<sup>3</sup>Faculty of Nuclear Engineering, University of Shahid Beheshti, Tehran, Iran

\*Corresponding author: Mehrdad.Ghalamchi.mech@gmail.com

Received November 01, 2013; Revised November 23, 2013; Accepted December 05, 2013

**Abstract** Renewable energies are playing a fundamental role in supplying energy, as these kinds of energies can be clean, low carbon and sustainable. Solar chimney power plant is a novel technology for electricity production from solar energy. A solar chimney power plant derives its mechanical power from the kinetic power of the hot air which rises through a tall chimney, the air being heated by solar energy through a transparent roof surrounding the chimney base. The performance evaluation of solar chimney power plant was done by FLUENT software by changing three parameters including collector slope, chimney diameter and entrance gap of collector. The results were validated with the solar chimney power plant which was constructed in Zanaj, Iran with 12 m height, 10 m collector radius and 10 degree Collector angle. By simulation and numerical optimization of many cases with dimensional variations, increasing 300 to 500 percent of chimney velocity and eventually increasing output power of system was observed in different cases.

**Keywords:** renewable energy, solar chimney, numerical simulation, Zanjan

**Cite This Article:** M. Ghalamchi, M. Ghalamchi, and T. Ahanj, "Numerical Simulation for Achieving Optimum Dimensions of a Solar Chimney Power Plant." *Sustainable Energy* 1, no. 2 (2013): 26-31. doi: 10.12691/rse-1-2-3.

## 1. Introduction

According to the shortage of the current energy resources and increasing the global energy demand and also, regarding to this reality that the energy obtained of the fossil fuels is environment damaging and nonrenewable, the demand of achieving a technology for exploitation of clean and renewable energies is sensed. Solar chimney power plant is one of the proper options for using the clean energy resources. The solar chimney technology is designed for preparing energy in large scales. In this type of power plant, the solar energy and subsequently the air movement are used. The air flow cause turbine rotation and the rotation is converted to electrical energy by a generator.

The conceptual design of solar chimney power plants was first propounded by professor Schaich in 1978 [1]. Before 1980, the system was built as an experimental sample in Manzanares, Spain [2]. The chimney diameter, collector radius, and height of the sample were 10 m, 122 m, and 194.6 m, respectively. The maximum output power of the system reached to 41 KW in September, 1982. Since then, many researchers became interested in this work and studied the related technologies for the high potential and vast applications of solar chimney power plants. Yan et al. [3] and Padki and Sherif [4] have done some of the Preliminary study on the thermo-fluid

analysis of a solar chimney power plant. In 1983, Krisst built a 10 W, 6 m collector diameter, 10 m height chimney in US [5]. In 1997, a chimney was built in Florida University and the plan was optimized for two times [6]. In aspect of small scales, a model with 0.14 W outlet power, 3.5 cm chimney radius, 2 m height, and 9 m<sup>2</sup> collector areas was built by Klink, Turkey [7].

Pretorius and Kröger [8], Ninic [9], Onyango and Ochieng [10] investigated the influence of a developed convective heat transfer equation, more accurate turbine inlet loss coefficient, quality of collector roof glass, and various types of soil on the performance of a solar chimney power plant. Ming et al. [11] evaluated the temperature and pressure fields for air in solar chimney power plant. More investigation and simulations have been carried out by Lodhi [12], Bernardes et al. [13], Bernardes et al. [14], von Backstro "mand Gannon [15], Gannon and von Backstro "m [16], Pastohr et al. [17], Schlaich et al. [18], Bilgen and Rheault [19].

The efficiency of solar chimney power plant was investigated according to the previous works. Since the practical measurements are much difficult, the simulation methods would be much easier for efficiency prediction of the different models of solar chimneys. Generally speaking, different combinations of chimney and collector dimensions can be built for purpose of electrical power production. Considering the cost reduction, that is much important that the optimized combination of chimney-collector dimensions would be known for the prediction.

In this paper, the mathematical model and experimental results of a solar chimney, which was built in University of Zanjan, are described.

## 2. Operation of Solar Chimney Power Plants

The solar chimney power plants include three main components: chimney, collector, and turbine generator. Chimney is a tall cylindrical structure which is equipped with turbine generator and installed on the middle of collector. The ground under the collector is covered by black bodies which are able to absorb the solar radiation energy. In general, collector is an enclosure which has one inlet and one exit, the collector inlet is the plant atmospheric air and the outlet is connected to the chimney base. The chimney can be installed vertically on the collector or may be laid as inclined on a mountain. This composition causes sunlight to convert to electrical energy and the conversion is divided to two stages. In the first stage, the conversion of solar energy to thermal energy which is done by using the thermal absorbers in the collector and the greenhouse effect increases the temperature. In the second stage, the chimney converts the thermal energy to kinetic energy and then is converted to electrical energy by a combination of wind turbine and generator. This energy conversion is done due to two reasons: the first reason is that the air temperature raising causes the air density decreasing, hence the air moves toward the chimney exit point, the second reason is the conic shape of the chimney which causes increasing the velocity of the air that move toward the center of the collector. The schematic of the chimney is shown in Figure 1.

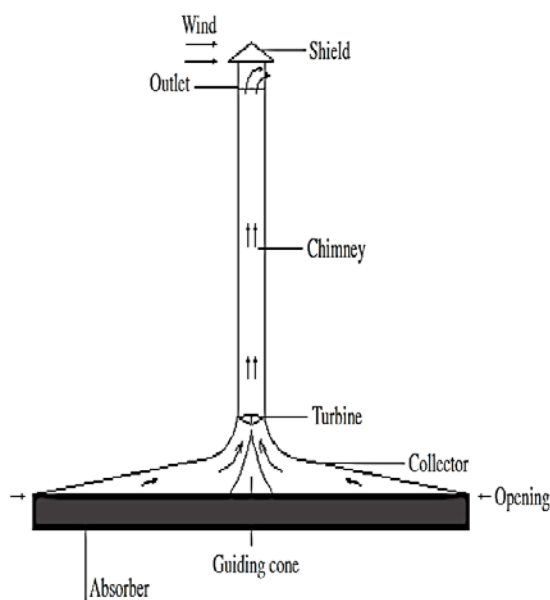


Figure 1. Schematic of the solar chimney

The collectors, in the simplest state, can be made of glass or transparent plastics which are located horizontally with a space from ground. The transparent layer is able to transmit the radiation from sun position (short wave-length waves), but in return the radiations emitted by ground (long wave-length waves) are trapped. Therefore,

the ground under the collector is warmed up and causes warming the radial air flow. The collectors were made of polycarbonate sheets, while the ground was covered by thick polyethylene black films. The polyethylene films play the role of absorbent which are able to store the heat during the day and reject it at night. Hence, an annual-permanent power generation may be obtainable.

The chimney is similar to a pressure pipe with low friction loss. The upward movement force of the warm air is dependent on the collector air temperature, air volumetric rate, and chimney height. The volumetric rate and air velocity rising makes better movement of the turbine and finally more electrical power. The air flow which passes through the turbine, can be adjusted by the turbine blade angle. The produced mechanical energy is converted to electrical energy by coupling the turbine with a generator.

A solar chimney doesn't need the direct insulation, the energy can even be supplied in cloudy days.

## 3. Solar Chimney Set-up

For purpose of more studies regarding these kinds of power plants, an experimental sample was built in University of Zanjan, in 2010 [20]. The chimney height is 12 m and the collector has 10 m diameter. The collector angle must be designed in a way that the most possible heat could be absorbed, Zanjan city has the attitude of  $36^\circ$ ,  $68'$  and longitude of  $48^\circ$ ,  $45'$  [21]. So if we want to have the most absorbed heat by the collector, the collector output must have the height of  $5 \tan \pi/6$ . The collector output was made with a height of 1m and the collector opening was 15 cm. The schematic and the dimensions of the built sample are shown in Figure 2 and Table 1.

Table 1. Dimensions of the built sample

Geometric parameter	Symbol	Amount (m)
Collector opening height	$H_2$	0.15
Collector output height	$H_c - H_2$	1
Chimney diameter	$d_c$	0.25
Collector diameter	$d_2$	10
Chimney height	$H_c$	12

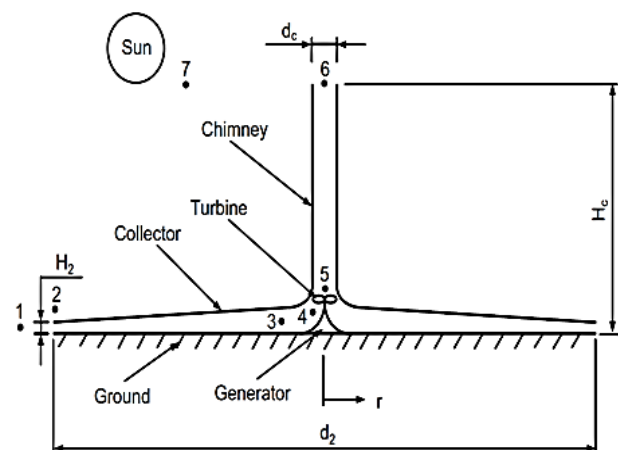


Figure 2. Schematic of the built model

Because of the UV resistance and proper cost of polyethylene, a 12 m length, 0.25 m diameter polyethylene pipe was used as the chimney. Due to the low diameter and height of the chimney, the friction inside the chimney is very low. The collector structure is made of 48 pieces of steel profiles, for strengthening the collector against wind and heavy snow a 4×4 steel profile was used and the collector bases was put into cement foundation. The greenhouse effect of the collector was supplied by the double-layer polycarbonate sheets. The grade of the material is UV resistant and the air between the sheet layers prevents heat loss. For temperature measuring in different zones of the power plant, SMT-160 sensors were utilized and a data-logger registered all the data round the clock. Totally, 12 temperature sensors were used for the measurements from which, 4 sensors were allocated for the chimney and 8 for the collector. The chimney sensors were positioned exactly at the middle with 3 m distances. Also, the collector sensors were put under the PC sheets with different height. Ambient temperature measuring was done using resistance sensors in 2 m height. An accurate anemometer, installed in 10 m height, was used for measuring the ambient wind velocity, and AVM-702 anemometer was utilized for measuring the air velocity inside the chimney at the opening. The photo of the power plant is shown in Figure 3.



Figure 3. Photo of the built solar chimney

In present study the performance evaluation of solar chimney power plant by changing three main parameters including collector slope, chimney diameter and entrance gap of collector in constant absorber of 78.5 m<sup>2</sup> investigated.

## 4. Governing Equation

Governing equations include the continuity equation, the Navier-Stokes equations, the energy equation and k-ε equations which are presented as followings:

Continuity equation:

$$\frac{\partial P}{\partial t} + \frac{1}{r} \frac{\partial}{\partial z} (r\rho u) + \frac{\partial}{\partial z} (\rho v) = 0 \quad (1)$$

Navier-Stokes equations:

$$\rho \frac{du}{dt} = -\frac{\partial P}{\partial r} + \frac{\partial}{\partial r} \left[ 2\mu \frac{\partial u}{\partial r} + \mu' \vec{\nabla} \cdot \vec{v} \right] + \frac{\partial}{\partial z} \left[ \mu \left( \frac{\partial u}{\partial z} + \frac{\partial v}{\partial r} \right) \right] + \frac{2\mu}{r} \left( \frac{\partial u}{\partial r} - \frac{v}{r} \right) \quad (2)$$

$$\rho \frac{dv}{dt} = -\frac{\partial P}{\partial z} + \rho g + \frac{\partial}{\partial z} \left[ 2\mu \frac{\partial v}{\partial z} + \mu' \vec{\nabla} \cdot \vec{v} \right] + \frac{1}{r} \frac{\partial}{\partial r} \left[ \mu r \left( \frac{\partial u}{\partial z} + \frac{\partial v}{\partial r} \right) \right] \quad (3)$$

Energy equation:

$$\rho c_p \left[ \frac{\partial T}{\partial t} + \frac{1}{r} \frac{\partial}{\partial r} (rTu) + \frac{\partial}{\partial z} (Tv) \right] = \frac{1}{r} \frac{\partial}{\partial r} \left( rw \frac{\partial T}{\partial r} \right) + \frac{\partial}{\partial z} \left( w \frac{\partial T}{\partial z} \right) + \frac{\partial P}{\partial t} + \frac{1}{r} \frac{\partial}{\partial r} (rPu) + \frac{\partial}{\partial z} (Pv) + \Phi \quad (4)$$

k-ε Equations:

$$\rho \left[ \frac{1}{r} \frac{\partial}{\partial r} (rku) + \frac{\partial}{\partial z} (kv) \right] = \frac{\partial}{\partial z} \left[ \left( \mu + \frac{\mu_t}{\sigma_k} \right) \frac{\partial k}{\partial z} \right] + \frac{1}{r} \frac{\partial}{\partial r} \left[ r \left( \mu + \frac{\mu_t}{\sigma_k} \right) \frac{\partial k}{\partial r} \right] + G_k + \beta g \frac{\mu_t}{Pr_t} \frac{\partial T}{\partial z} - \rho \epsilon \quad (5)$$

$$\rho \left[ \frac{1}{r} \frac{\partial}{\partial r} (r\epsilon u) + \frac{\partial}{\partial z} (\epsilon v) \right] = \frac{\partial}{\partial z} \left[ \left( \mu + \frac{\mu_t}{\sigma_\epsilon} \right) \frac{\partial \epsilon}{\partial z} \right] + \frac{1}{r} \frac{\partial}{\partial r} \left[ r \left( \mu + \frac{\mu_t}{\sigma_\epsilon} \right) \frac{\partial \epsilon}{\partial r} \right] + C_{1\epsilon} G_k \frac{\epsilon}{k} - C_{2\epsilon} \rho \frac{\epsilon^2}{k} \quad (6)$$

Assuming one-dimensional, steady state flow, the following equation would be valid for mass flow rate:

$$\dot{m} = \rho_f AU_f \quad (7)$$

Substituting flow cross section area in equation (1) yields in:

$$U_f = -\frac{\dot{m}}{2\pi r H_c \rho_f} \quad (8)$$

The energy equation of the hot air inside the collector is:

$$\rho_a C_p U_f H_c \frac{\partial T_f}{\partial r} = h_c (T_f - T_c) + h_e (T_f - T_e) \quad (9)$$

In this form of energy equation, the conduction heat transfer includes all the connecting surfaces. For finding the temperature of the surfaces, we need integration of equation (3). At first, a preliminary amount is assumed for the surfaces temperature and heat transfer coefficient. Assuming constant amount for the air density, substituting  $U_f$  of equation (2) in (3), and then integrating equation (3), the following simplified correlation is obtained:

$$T_f(r) = \frac{1}{2} \left[ T_c + T_e + (2T_a - T_c - T_e) e^{\frac{2\pi h}{C_p \dot{m}} (r^2 - r_0^2)} \right] \quad (10)$$

The collector inlet air flow profile in a given mass flow rate is depicted in Figure 3. For proving the effect of the surface temperatures on the temperature profile of the fluid, three different amounts are selected for the ground and collector ceiling temperatures. Considering  $\dot{m}=10$  kg/s and  $h=5$  W/m<sup>2</sup>K, equation for is solved for constant wall temperature conditions. Figure 4 shows the temperature rising of the collector entered air. The temperature difference between the collector inlet and outlet shows the vertical efficiency of the system. The results demonstrate that the temperature between the inlet and outlet is increased by raising the temperatures of the ground and collector surface, so that, this temperature increase causes the system efficiency promotion.

Therefore, the energy equation of the collector air may be revised as:

$$\rho_a C_p u_f H_c \frac{\partial T_f}{\partial r} = h_c (T_f - T_c(r)) + h_e (T_f - T_e(r)) \quad (11)$$

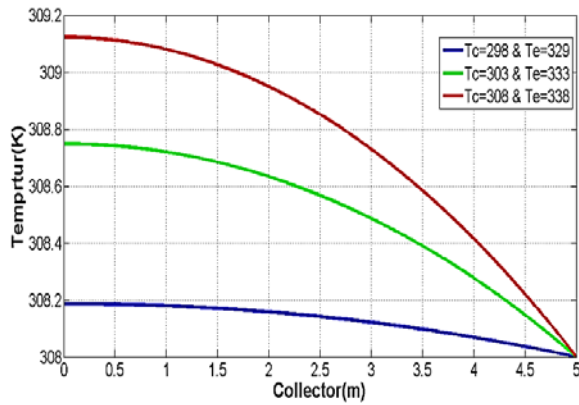


Figure 4. The temperature profile of the fluid flow along with collector  $\dot{m} = 10 \text{ kg s}^{-1}$

## 5. Numerical Simulation of System

In this part of the study, the numerical simulation of the solar chimney power plant is presented. A physical model for a solar chimney power plant was built based on the geometrical dimensions of the prototype of Zanjan. The basic equations including the models discussed up to now were numerically solved with the help of the commercial simulation program FLUENT (6.3). The basic equations

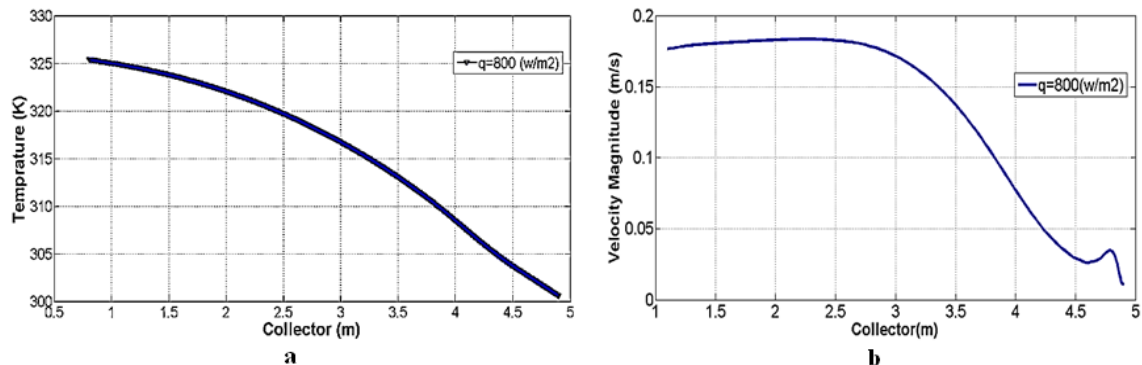


Figure 6. Collector temperature distribution

were simplified to axisymmetric and steady state. Because a turbulence model is necessary for the description of the turbulent flow conditions, the standard k- $\epsilon$  model and standard wall mode were selected to describe the fluid flow inside the collector and the chimney. The domain was discretized with 45,000 two-dimensional unstructured mesh elements. The grid was refined adaptively (hanging nodes) near walls (bend, glass, ground and chimney) and in the area of the turbine. This is required because large gradients appear near the walls. Boundary conditions of zanjan solar chimney power plant indicate at Figure 5 and Table 2.

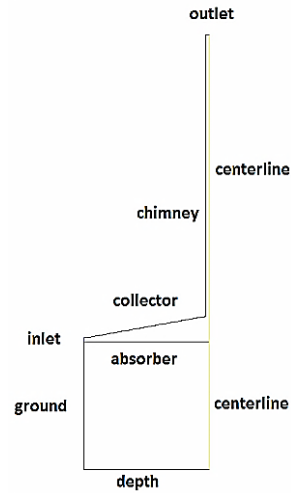


Figure 5. Boundaries locations

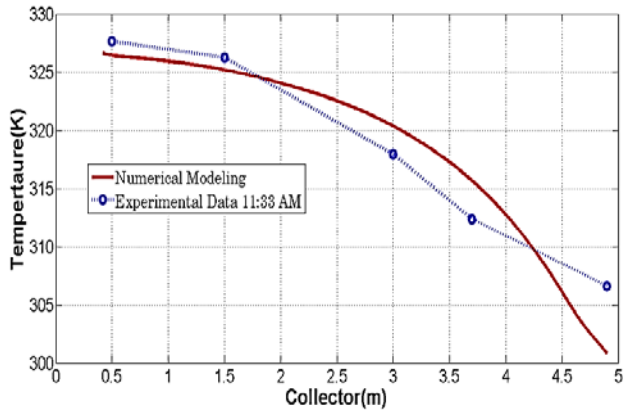
Table 2. Boundary Condition

Material	Boundary Condition		
	Boundary	Type	Condition
Fluid (Air)	Centerline	Axis	Symmetry axis
	Absorber	Wall	Convective heat transfer
	Collector	Wall	Convective heat transfer
	Chimney	Wall	Insulated surface
	Inlet	Pressure inlet	Atmospheric pressure
	Outlet	Pressure outlet	Atmospheric pressure
Solid (Soil)	Centerline	Axis	Symmetry axis
	Absorber	Wall	Convective heat transfer
	Ground	Wall	Insulated surface
	Depth	Wall	Constant temperature

All numerical calculations had to be carried out with the solver with double precision. The iteration error was at least  $10^{-6}$  on all calculations, for the energy equation at least  $10^{-9}$ . Under these conditions, the solution converged in less than 2500 iterations. Figure 6 a. shows the collector temperature distribution and 6 b. velocity magnitude for  $800 \text{ (w/m}^2\text{)}$  with ambient temperature of 300 k.

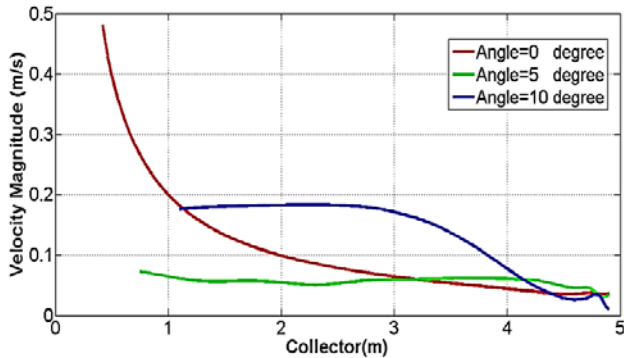
## 6. Results and Discussion

Figure 7 compares the experimental and numerical collector temperature distribution over 9 cm of absorber at 11:33 AM.

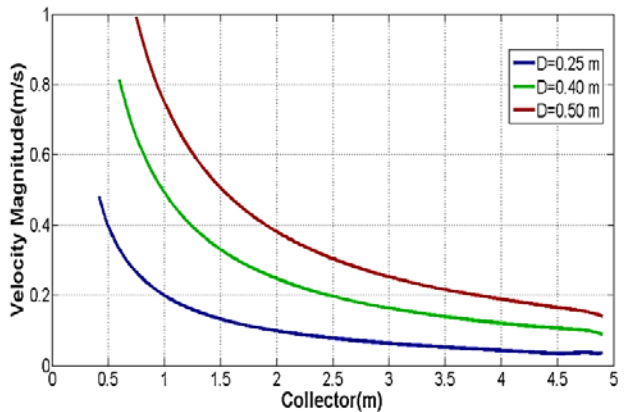


**Figure 7.** Experimental and numerical collector temperature distribution over 9 cm of absorber

Compare experimental and numerical results shows the good agreement. Figure 8 indicates the velocity magnitude distribution in collector with 0.15m inlet, 0.25m chimney diameter and with slope of 0,5,10 degrees over 9 cm of absorber.



**Figure 8.** Velocity magnitude distribution of collector for different collector slope



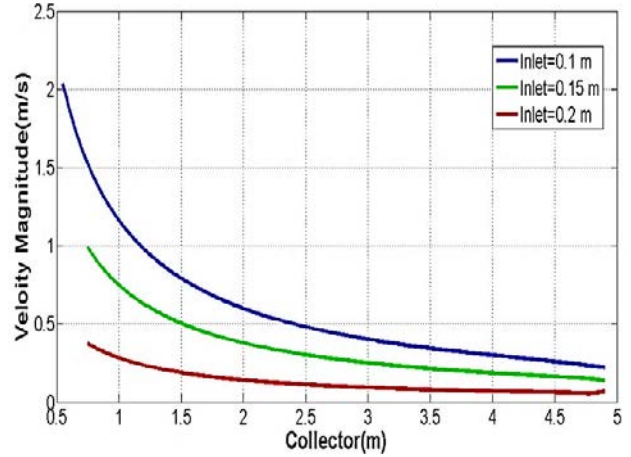
**Figure 9.** Velocity magnitude distribution of collector for different chimney diameter

Figure 8 appears the best angle of collector is zero. Because the air flow in the collector with collector slope of zero move in the straight stream lines and in the

turbulent regime of the air flow the eddy generation comes down. Figure 9 indicate the velocity magnitude distribution in collector with 0.15m inlet, zero collector slope and chimney diameter of 0.25,0.4 and 0.5 m over 9 cm of absorber.

Figure 9 shows the best diameter of chimney is 0.5 m for special constant of zanjan solar chimney absorber.

Figure 10 shows the best entrance height of collector is 0.1 m for special constant of Zanjan solar chimney absorber Figure 8, Figure 9 and Figure 10 indicates that the velocity magnitude of Zanjan Solar chimney power plant can improve 300 to 500 percent in different cases.



**Figure 10.** Velocity magnitude distribution of collector for different entrance height

## 7. Conclusion

In present study, the collector of Zanjan Solar chimney power plant mathematically modeled. The numerical model of collector validate with experimental data of temperature sensors. The performance evaluation of solar chimney power plant was done by FLUENT software by changing three parameters including collector slope, chimney diameter and entrance gap of collector. The results shows that the horizontal collector works better and the best chimney diameter and entrance gap of collector are 0.5 and 0.1 m respectively. By simulation and numerical optimization of many cases with dimensional variations, increasing 300 to 500 percent of chimney velocity and eventually increasing output power of system was observed in different cases.

## Nomenclature

$c_p$	Specific heat capacity (J/kg.K)
$D$	Diameter (m)
$h$	Convective heat transfer coefficient (W/m <sup>2</sup> .K)
$\dot{m}$	Mass flow rate (kg/s)
$P$	Pressure (Pa)
$r$	Radial coordinate (m)
$T$	Temperature (K)
$u$	Velocity in the radial direction (m/s)
$V$	Quantity of velocity vector (m/s)
$v$	Velocity in the axial direction (m/s)
$w$	Thermal conductivity (W/m.K)

$z$	Axial coordinate (m)
$\beta$	Thermal expansion coefficient (1/K)
$\rho$	Density (kg/m <sup>3</sup> )

**Subscripts**

$a$	Ambient
$e$	Absorber
$c$	Collector
$ch$	Chimney
$i$	Inner
$o$	Out
$r$	Radial coordinate

**References**

- [1] Bernardes, M.A., dos, S., Voss, A., Weinrebe, G. *Thermal and technical analyzes of solar chimneys*. Solar Energy 2003, 511-524.
- [2] Haaf, W. Solar chimneys: part ii: preliminary test results from the Manzanares pilot plant. *Solar Energy* 14 (2), 141-161. May.1984.
- [3] Yan, M.Q., Sherif, S.A., Kridli, G.T., Lee, S.S., Padki, M.M., 1991. Thermo-fluid analysis of solar chimneys. In: Morrow, T.B., Marshall, L.R., Sherif, S.A. (Eds.), *Industrial Applications of Fluid Mechanics-1991*, FED, vol 132. The American Society of Mechanical Engineers, New York, pp. 125-130.
- [4] Padki, M.M., Sherif, S.A., 1999. On a simple analytical model for solar chimneys. *Energy Research* 23 (4), 345-349.
- [5] Krisst, R.J.K., 1983. *Energy transfer system. Alternative Source Energy* 63, 8-11.
- [6] Pasumarthi N, Sherif SA. *Experimental and theoretical performance of ademon- stration solar chimney model—Part II: experimental and theoretical results and economic analysis*. Int J Energy Res 1998; 22:443-61.
- [7] Klink, H., 1985. *A prototype solar convection chimney operated under Izmit conditions*. In: *Proceedings of the 7th Miami International Conference on Alternative Energy Sources*, Veiroglu, TN, vol. 162.
- [8] Pretorius JP, Kröger DG. Critical evaluation of solar chimney power plant per- formance. *Sol Energy* 2006; 80:535-44.
- [9] Ninic N. Available energy of the air in solar chimneys and the possibility of its ground-level concentration. *Sol Energy* 2006; 80:804-11.
- [10] Onyango FN, Ochieng RM. *The potential of solar chimney for application in rural areas of developing countries*. Fuel 2006; 85:2561-6.
- [11] Ming, T., Liu, W., Xu, G., 2006. *Analytical and numerical investigation of the solar chimney power plant systems*. Int. J. Energy Res. 30 (11), 861-873.
- [12] M.A.K. Lodhi, *Application of helio-aero-gravity concept in producing energy and suppressing pollution*, Energy Convers. Manage. 40(1999) 407-421.
- [13] M.A. dos S Bernardes, A. Vob, G. Weinrebe, *Thermal and technical analyzes of solar chimneys*, Sol. Energy 75 (2003) 511-524.
- [14] M.A. dos S Bernardes, R.M. Valle, M.F. Cortez, *Numerical analysis of natural laminar convection in a radial solar heater*, Int. J. Therm.Sci. 38 (1999) 42-50.
- [15] T.W. Von Backstro'm, A.J. Gannon, *Compressible flow through solarpower plant chimneys*, ASME J. Sol. Energy Eng. 122 (2000) 138-145.
- [16] A.J. Gannon, T.W. von Backstro'm, *Solar chimney turbine performance*, ASME J. Sol Energy Eng. 125 (1) (2003) 101-106.
- [17] H. Pastohr, O. Kornadt, K. Gurlebeck, *Numerical and analytical calculations of the temperature and flow field in the upwind power plant*, Int. J. Energy Res. 28 (2004) 495-510.
- [18] J. Schlaich, R. Bergermann, W. Schiel, G. Weinrebe, *Design ofcommercial solar updraft tower systems-utilization of solar inducedconvective flows for power generation*, ASME J. Sol. Energy Eng. 127(2005) 117-124.
- [19] E. Bilgen, J. Rheault, *Solar chimney power plants for high latitudes*, Sol. Energy 79 (2005) 449-458.
- [20] Kasaecian, A.B., Heidari, E., NasiriVatan, Sh., 2010. *Experimental investigation of climatic effects on the efficiency of a solar chimney pilot power plant*. *Renewable and Sustainable Energy Reviews* 20 (8). 5202-5206.
- [21] Sabziparvar AA, Shetaee H. *Estimation of global solar radiation in arid and semi- arid climates of east and west Iran*. 2007, 32-55.